Performance Comparison of Several Algorithms for Localization of Wideband Sources

Hassan Ougraz, Said Safi, Ahmed Boumezzough, Miloud Frikel

Performance Comparison of Several Algorithms for Localization of Wideband Sources

Hassan Ougraz[1], Said Safi[1], Ahmed Boumezzough[1], and Miloud Frikel[2]

[1] *University of Sultan Moulay Slimane Beni Mellal, Morocco,*
[2] *National Graduate School of Engineering and Research Center Caen, France*

https://doi.org/10.26636/jtit.2023.3.1359

Abstract — In recent years, researchers have tried to estimate the direction-of-arrival (DOA) of wideband sources and several novel techniques have been proposed. In this paper, we compare six algorithms for calculating the DOA of broadband signals, namely coherent subspace signal method (CSSM), two-sided correlation transformation (TCT), incoherent multiple signal classification (IMUSIC), test of orthogonality of frequency subspaces (TOFS), test of orthogonality of projected subspaces (TOPS), and squared TOPS (S-TOPS). The comparison is made through computer simulations for different parameters, such as signal-to-noise ratio (SNR), in order to establish the efficiency and performance of the discussed methods in noisy environments. CSSM and TCT require initial values, but the remaining approaches do not need any preprocessing.

Keywords — coherent, DOA estimation, incoherent, localization, wideband sources

1. Introduction

Many applications rely on sensor arrays. These include radar signal processing [1]–[3], sonar, medical imaging, wireless communication systems [4]–[7], and Internet of Things [8]–[10]. In the simplest scenario, signals received by the sensors are scaled and contain delayed replicas of the waveform emitted by a single source. In a complex case, numerous sources and multiple propagation pathways from the sources to the sensors may exist. In the Fourier domain, the most frequent strategy is to decompose the broadband source into narrowband elements [11]–[12]. Moreover, localization of wideband sources is primarily based on figuring out how to employ numerous covariance matrices at various frequencies to construct precise DOA estimation [11], [13]. A variety of approaches have been suggested to fix the problem of the direction-of-arrival (DOA) estimation of various broadband signals. These are categorized as incoherent signal subspace algorithms [14], [15] and coherent signal subspace algorithms [16], [17].

In this paper, we discuss the capabilities of some algorithms used for estimating the location of wideband signal sources. Being one of the fundamental wideband DOA estimation methods, incoherent methods rely on numerous narrowband sources that have been incoherently extracted from a broadband source [18]. In particular, these techniques apply independently narrowband approaches, such as multiple signal classification (MUSIC) [19], to signal sources. The first approach is incoherent MUSIC (IMUSIC). Its prediction resolution improves in high signal-to-noise ratio (SNR) zones and degrades when the SNR of several frequencies is minimal. Moreover, weak estimations from several bands of frequencies will have an impact on the performance of the overall estimation. The second approach is the test of orthogonality of frequency subspaces (TOFS) [20] which generates steering vectors for each DOA and frequency available. When SNR is high, the estimation accuracy is quite good, since TOFS is an incoherent technique [20]. However, when SNR is low, TOFS is unable to resolve the desired DOAs. Another algorithm, known as the test of orthogonality of projected subspaces (TOPS) [21], applies the signal and noise subspaces of various frequencies to offer better DOA estimation performance without the requirement to provide any starting values. Thus, TOPS fills the gap between coherent and incoherent methods. This technique offers the following advantages [21]:

- it does not require a beamforming matrix or focusing angles,
- when SNR is high, it is not biased,
- at low SNR, it merges frequency bands more efficiently than incoherent approaches.

The drawback of such an approach is that it is challenging to determine the real DOA of sources, since the spatial spectra computed using the TOPS method contain several incorrect lobes. The squared TOPS (S-TOPS) approach [28] employs the signal subspace and noise subspace twice and achieves the squared test of orthogonality of both subspaces. S-TOPS outperforms TOPS at small SNR values, since its resolution has been enhanced.

The coherent signal subspace method (CSSM) has been suggested to resolve these drawbacks and to estimate DOA [16]. The covariance matrix of each frequency band is focused by transformation arrays and the focusing arrays are averaged to produce a novel covariance matrix in the coherent signal subspace approaches. The main point of this approach is to precisely focus these covariance matrices. The two-sided correlation transformation (TCT) approach, an alternative of CSSM, is proposed to improve performance.

Various approaches for extracting a proper focusing array have been suggested, e.g. in [23], [24]. Nevertheless, each focusing algorithm entails starting values which are the predetermined angles of arriving sources, and the efficiency of coherent signal subspace methods is related to an initial value [25].

In this paper, we concentrate on the comparison of the techniques mentioned above, with various SNR values, different snapshots and for various angles of sources, in order to provide a more accurate comparison in terms of the advantages and drawbacks of these approaches. The remaining part of this paper has the following structure. In Section 3, the wideband model and the problem of localization will be investigated. The wideband methods are investigated in Section 4, while the experimental results are discussed in Section 5. Finally, Section 6 presents the conclusions and future outlooks.

2. Related Works

Many papers focusing on localization and wideband DOA estimation for incoherent sources are closely related to our work in this domain. The first is [13] as it proposes a novel approach to estimating the wideband sources, namely weighted squared TOPS, and confirms that it outperforms other methods. Paper [13] does something similar to this specific work. However, we present a comparative study using IMUSIC, TOFS, TOPS, S-TOPS, CSSM, and TCT to estimate the wideband sources, and to determine which one of them performs the best. Additionally, the comparative study of three wideband DOA estimation algorithms (TCT, TOPS, W-CMSR), as presented in [11], demonstrates that W-CMSR surpasses both TCT and TOPS in terms of resolution capability.

3. Problem Formulation

The M elements of a uniform linear array (ULA) are evenly spaced, with the distance d between succeeding elements being no more than half of the wavelength. We assume that L wideband sources ($L < M$) are either known or can be determined [26] and are impinging on the array elements from different angles $(\theta_1, \theta_2, \ldots, \theta_L)$. Figure 1 shows the ULA geometry for the localization of broadband signals.

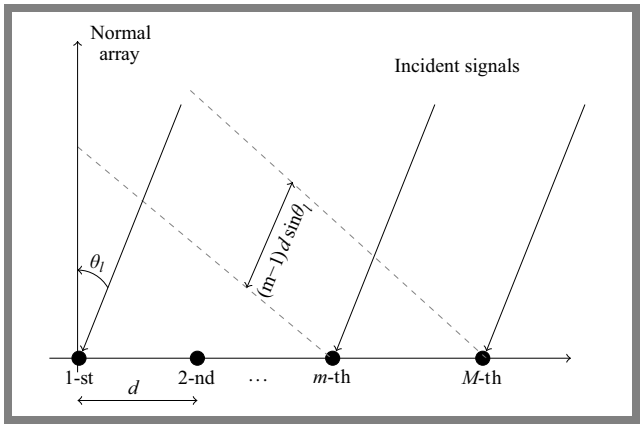

Fig. 1. ULA geometry of M antennas [11].

Our goal is to estimate the direction of arrival of L wideband sources using an ULA of M antennas supposing that all sources are uncorrelated and occur in the bandwidth between the smallest ω_s and the largest ω_L source frequency. Thus, the received data at the *m*–th antenna are given as follows:

$$x_m(t) = \sum_{l=1}^{L} s_l(t - v_m \sin\theta_l) + n_m(t)\,, \tag{1}$$

where $s_l(t)$ is the *l*–th source, $n_m(t)$ is an additive white Gaussian noise (AWGN) at the *m*–th component, $v_m = (m-1)d/c$, where d is the distance between the components of ULA, and c is the velocity of light. θ_l is the angle to be computed. The received data is split into K narrowband signals. Thus, the discrete Fourier transform (DFT) of the received signals at *m*–th element is:

$$x_m(\omega) = \sum_{l=1}^{L} s_l(\omega)\mathrm{e}^{-\mathrm{j}\omega v_m \sin\theta_l} + n_m(\omega)\,. \tag{2}$$

The DFT output signals can then be represented in vector form [11]:

$$x(\omega_i) = A(\omega_i, \theta)s(\omega_i) + n(\omega_i),\ i = 1, 2, \ldots, K\,, \tag{3}$$

where $\omega_S < \omega_i < \omega_L$ for $i = 1, 2, \ldots, K$,

$$A(\omega_i, \theta) = [a(\omega_i, \theta_1)\ \ a(\omega_i, \theta_2)\ \ \ldots\ \ a(\omega_i, \theta_L)]\,, \tag{4}$$

$$a(\omega_i, \theta_l) = \begin{bmatrix} 1 \\ \mathrm{e}^{-\mathrm{j}\omega_i v_1 \sin\theta_l} \\ \vdots \\ \mathrm{e}^{-\mathrm{j}\omega_i v_{M-1} \sin\theta_l} \end{bmatrix}\,, \tag{5}$$

where T is the transpose of a given matrix.

The correlation matrix is calculated in the following manner [11]:

$$\begin{aligned} R_{xx}(\omega_i) &= E[x(\omega_i)x^H(\omega_i)] \\ &= A(\omega_i, \theta)R_{ss}(\omega_i)A^H(\omega_i, \theta) + \sigma_n^2 I\,, \end{aligned} \tag{6}$$

where $E[.]$ is the expectation value operator, H is the Hermitian operator, $R_{ss}(\omega_i) = E[s(\omega_i)s^H(\omega_i)]$, σ_n^2 is the noise power, and I is the $M \times M$ unit matrix. Supposing that $R_{ss}(\omega_i)$ has a complete rank, the signal subspace $F_s(\omega_i)$ and the noise subspace $F_n(\omega_i)$ matrices at the frequency ω_i can be generated using the eigen-values decomposition (EVD) or the singular value decomposition (SVD) of the correlation array as:

$$F_s(\omega_i) = [e_1(\omega_i), e_2(\omega_i), \ldots, e_L(\omega_i)]\,, \tag{7}$$

$$F_n(\omega_i) = [e_{L+1}(\omega_i), e_{L+2}(\omega_i), \ldots, e_M(\omega_i)]\,, \tag{8}$$

where $e_1(\omega_i), \ldots, e_M(\omega_i)$ are the perpendicular eigenvectors of $R_{xx}(\omega_i)$, ranked in decreasing order by their corresponding eigen-values as follows:

$$\lambda_1(\omega_i) \geqslant \ldots \geqslant \lambda_L(\omega_i) \geqslant \lambda_{L+1}(\omega_i), \ldots, \lambda_M(\omega_i) = \sigma_n^2\,. \tag{9}$$

4. Wideband Algorithms

In this part, we investigate several techniques for localization of broadband signals. As described in Section 3, DFT is used to break down every wideband source into K narrowband signals.

4.1. Coherent Signal Subspace Method (CSSM)

Many strategies have been proposed to address the drawbacks of incoherent methods by finding a good way to integrate the signal subspaces coherently into one general correlation matrix in which narrowband high-resolution methods may be used. CSSM, proposed by Wang and Kaveh [27], was the first technique to coherently sum the correlation matrices of different frequency bins [27]. It converts the correlation matrices at many frequency bins into a single general correlation matrix at a single focusing frequency using a frequency-dependent transformation matrix (focusing matrix). The focusing matrix F is intended to provide the solution to the following equation:

$$F_i A_i = A_0, \qquad i = 1, \ldots, K\,. \tag{10}$$

To estimate the angles-of-arrival that may be employed to generate A_0, a pre-process is required. The observation vectors at different frequency bins are converted into the focusing subspace using the focusing matrices. The standard proposed in [27] is based on the transformation matrices produced from the constrained minimization problem:

$$\begin{cases} \min_{F_i} \mid\mid A_0 - F_i A_i \mid\mid \\ F_i^H F_i = I \end{cases}. \tag{11}$$

Hung *et al.* established in [14] that the focusing matrix that solves the problem given by Eq. (11) is:

$$F_i^{CSSM} = V_i W_i^H\,. \tag{12}$$

where $V_i \Sigma_i W_i$ is the singular values decomposition of $A_0 A_i^H$. Following the determination of the focusing matrix, a high resolution approach such as MUSIC [19] is employed to determine the DOAs. The DOAs are calculated by determining the angular position of peaks in the MUSIC algorithm's spatial spectrum.

Algorithm 1. CSSM algorithm.

1: Use an ordinary beamformer to scan the space and find an initial estimate of the DOAs.
2: Apply a DFT to the array output to sample the spectrum of data.
3: For $i = 1, 2, \ldots, K$ **do**
4: Calculate the correlation matrix R_{xx} of every frequency ω_i.
5: End for
6: For $i = 1, 2, \ldots, K$ **do**
7: Determine the focusing matrices by using the Eq. (12).
8: End for
9: Apply MUSIC or any other high-resolution spectral estimation method to find the DOAs.

4.2. TCT Method

Two-sided correlation transformation (TCT) [29] is similar to CSSM introduced by Hung *et al.* in that signal subspaces are transformed using focusing matrices. The TCT transforms the correlation matrix using a two-sided unitary transformation. Let us consider the covariance matrix at the i–th frequency band in a noise-free floor:

$$P_i = A_i R_{ss}(\omega_i) A_i^H, \tag{13}$$

and P_0 is the focusing noise free covariance matrix. The TCT focusing matrices can be found by solving the minimization problem:

$$\begin{cases} \min_{F_i} \mid\mid P_0 - F_i P_i F_i^H \mid\mid \\ F_i^H F_i = I \end{cases}. \tag{14}$$

It is shown in [29] that the optimal solution of the problem is given by the eigenvectors of the covariance matrix at the frequencies ω_0 and ω_k as:

$$F_k^{TCT} = V_0 V_i^H\,, \tag{15}$$

where V_0 and V_i are the eigenvector matrices of P_0 and P_i, respectively.

Algorithm 2. TCT algorithm.

1: Use an ordinary beamformer to scan the space and find an initial estimate of the DOAs.
2: Split the data into K blocks of the same size.
3: Apply a DFT to the array output to sample the spectrum of data.
4: For $i = 1, 2, \ldots, K$ **do**
5: Calculate the correlation matrix R_{xx} of every frequency ω_i.
6: Form A_i, and S_i, using the results of the preprocessing step and Eq. (14).
7: End for
8: Average the source correlation matrices to obtain S_0 as in [30].
9: Find $P_0 = A_0 S_0 A_0^H$.
10: For $i = 1, 2, \ldots, K$ **do**
11: Calculate P_i by using Eq. (13).
12: End for
13: Determine the unitary transformation matrices.
14: Multiply these matrices by the sample correlation matrices, and average the results.
15: Apply MUSIC or any other high-resolution spectral estimation method to find the DOAs.
16: To improve the performance, iterate steps 3 to 5.

4.3. IMUSIC Approach

Because the narrowband MUSIC technique is used for all frequencies simultaneously, this approach is known as incoherent

MUSIC (IMUSIC) [13] and is considered to be one of the most fundamental DOA estimation techniques for wideband signals. Thus, IMUSIC calculates the DOA of broadband signals using the following formula:

$$\hat{\theta} = arg\ \min_{\theta} \sum_{i=1}^{K} a^H(\omega_i, \theta) F_n(\omega_i) F_n^H(\omega_i) a(\omega_i, \theta)\ , \quad (16)$$

where $F_n(\omega_i)$ is the noise subspace at every frequency ω_i. The noise subspace array $F_n(\omega_i)$ is obtained from the covariance matrix $R_x x(\omega_i)$ [21]. As long as the DOAs computed by Eq. (16), IMUSIC results are the averages of the outcomes of each range of frequencies. Weak estimations from one frequency range degrade the overall estimation accuracy.

Algorithm 3. IMUSIC algorithm.

1: Split the data into K blocks of the same size.
2: Calculate the DFT of the K blocks.
3: For $i = 1, 2, \ldots, K$ **do**
4: Calculate the correlation matrix R_{xx} of every frequency ω_i.
5: End for
6: For $i = 1, 2, \ldots, K$ **do**
7: Calculate the noise subspace $F_n(\omega_i)$ of each frequency ω_i by EVD/SVD of R_{xx}.
8: End for
9: Estimate the final DOA $\hat{\theta}$ using the Eq. (16).

IMUSIC is generally effective in noisy environments, and when the signals are well separated from one to another. However, when the SNR is low, it suffers from failures and generates side lobes at erroneous directions, which occurs in many situations. Additionally, the noise level is expected to be uniform across the band of frequencies, which is not usual [21]. The limitations of incoherent approaches encouraged the development of coherent approaches that are capable of addressing these drawbacks.

4.4. TOFS Approach

For each frequency, the TOFS approach utilizes the noise subspace created by the EVD/SVD of the covariance matrix [20]. To compute the DOA of every arriving broadband signal, TOFS relies on orthogonality between the steering array and the noise subspace. Since represents the single DOA of arriving broadband signals, then θ satisfies the formula [30]:

$$a^H(\omega_i, \theta) F_n(\omega_i) F_n^H(\omega_i) a(\omega_i, \theta) = 0\ . \quad (17)$$

The vector $D_i(\theta)$ is defined as [13]:

$$D_i(\theta) = \begin{bmatrix} a^H(\omega_1, \theta) F_n(\omega_1) F_n^H(\omega_1) a(\omega_1, \theta) \\ a^H(\omega_2, \theta) F_n(\omega_2) F_n^H(\omega_2) a(\omega_2, \theta) \\ \vdots \\ a^H(\omega_K, \theta) F_n(\omega_K) F_n^H(\omega_K) a(\omega_K, \theta) \end{bmatrix}^T . \quad (18)$$

Since the DOA of arriving broadband sources is θ, all elements of the vector $D_i(\theta)$ are zero.

Algorithm 4. TOFS algorithm [20].

1: Split the data into K blocks of the same size.
2: Calculate the DFT of the K blocks.
3: For $i = 1, 2, \ldots, K$ **do**
4: Calculate the correlation matrix R_{xx} of every frequency ω_i.
5: End for
6: For $i = 1, 2, \ldots, K$ **do**
7: Calculate the noise subspace $F_n(\omega_i)$ of each frequency ω_i by EVD/SVD of R_{xx}.
8: Generate $D_i(\theta)$ by Eq. (18) for each hypothesized DOA θ.
9: End for
10: Estimate the final DOA $\hat{\theta}$ by:

$$\hat{\theta} = arg\ \max_{\theta} \frac{1}{\sigma_{min}(\theta)}\ . \quad (19)$$

where $\sigma_{min}(\theta)$ is the shortest singular value of $D_i(\theta)$.

By employing the noise subspaces derived from the covariance matrix, TOFS offers better DOA estimation in noisy environments. However, when the SNR is low TOFS is unable to resolve closely spaced targets.

4.5. TOPS Approach

TOPS calculates the DOA of arriving broadband sources by employing the signal subspace and noise subspace of each frequency range [21]. The first step is to extract the signal subspace $F_s(\omega_i)$ and the noise subspace $F_n(\omega_i)$ from the EVD/SVD of the covariance array of each range of frequencies. Thus, one range of frequencies ω_i should be opted, and the signal subspace $F_s(\omega_i)$ of the opted range should be transformed into other bands. A diagonal unitary transformation array is used by TOPS. The *m*–th component on the diagonal of the frequency transform array $\Psi(\omega_i, \theta)$ is defined as:

$$[\Psi(\omega_i, \theta)]_{(m,m)} = \mathrm{e}^{-\mathrm{j}\omega_i \frac{md}{c} \sin\theta}\ . \quad (20)$$

The signal subspace $F_s(\omega_i)$ of the band of frequencies ω_i is transformed into the other frequency band ω_j by using $\Psi(\omega_i, \theta)$, where the transformed signal subspace $U_{ij}(\theta)$ is [21]:

$$U_{ij}(\theta) = \Psi(\Delta\omega, \theta) F_s(\omega_i),\ i \neq j\ , \quad (21)$$

where $\Delta\omega = \omega_j - \omega_i$.
The Eq. (21) can be written as follows:

$$\begin{aligned} U_{ij}(\theta) &= \Psi(\Delta\omega, \theta) A(\omega_i, \theta) G_i \\ &= A(\omega_j, \hat{\theta}) G_i\ , \end{aligned} \quad (22)$$

where $\hat{\theta}$ is the converted θ by using the frequency transform matrix $\Psi(\omega_i, \theta)$, and G_i is a complete rank square array that proves $F_s(\omega_i) = A(\omega_i, \theta) G_i$. An array manifold at any frequency and direction can be converted into another array

manifold at a different frequency by using this transformation process. Consequently, the transformed matrix has a complete rank and can be employed in the following orthogonality test between transformed array and noise subspace, investigated in detail in [21]. Given that the frequency range of relevance is ω_1, the estimator $D'(\theta)$ is given as [30]:

$$D_i'(\theta) = \begin{bmatrix} U_{12}^H(\theta)F_n(\omega_2) \\ U_{13}^H(\theta)F_n(\omega_3) \\ \vdots \\ U_{1K}^H(\theta)F_n(\omega_K) \end{bmatrix}^T . \tag{23}$$

When θ is one of the arriving wideband signals, the rank of the matrix $D_i'(\theta)$ also degrades same as TOFS. The performance of DOA estimation is dictated by the correctness of generating the covariance array, that is largely determined by the number of snapshots and the SNR of the received data. TOPS employs the subspace projection strategy to decrease leakage of signal subspace components in the predicted noise subspace. The projection array $P_i(\theta)$ is then computed as [30]:

$$P_i(\theta) = I - \left(a^H(\omega_i,\theta)a(\omega_i,\theta)\right)^{-1} a(\omega_i,\theta)a^H(\omega_i,\theta) , \tag{24}$$

where I is an $M \times M$ identity matrix. The noise robust matrix $D''(\theta)$ is obtained by substituting the component $U_{ij}(\theta)$ of Eq. (23) with a novel transformed signal subspace array $U_{ij}(\theta)$.

$$U_{ij}'(\theta) = P_j(\theta)U_{ij}(\theta) , \tag{25}$$

$$D_i''(\theta) = \begin{bmatrix} U_{12}^{'H}(\theta)F_n(\omega_2) \\ U_{13}^{'H}(\theta)F_n(\omega_3) \\ \vdots \\ U_{1K}^{'H}(\theta)F_n(\omega_K) \end{bmatrix}^T . \tag{26}$$

Since the projection matrix $P_i(\theta)$ eliminates subspace prediction errors, TOPS shows better performance when the Eq. (26) with $D_i''(\theta)$ is used.

Algorithm 5. TOPS algorithm [21].

1: Split the data into K blocks of the same size.
2: Calculate the DFT of the K blocks.
3: For $i = 1, 2, \ldots, K$ **do**
4: Select $x(\omega_i)$ at preselected ω_i.
5: Calculate the correlation matrix R_{xx} of every frequency ω_i.
6: End for
7: For $i = 1, 2, \ldots, K$ **do**
8: Calculate the signal subspace $F_s(\omega_1)$.
9: Compute the noise subspace $F_n(\omega_i)$ by EVD/SVD of the calculated correlation matrix R_{xx}.
10: Generate $D_i''(\theta)$ using Eqs. (25) and (26) for each hypothesized DOA θ.
11: End for
12: Estimate the final DOA $\hat{\theta}$ by

$$\hat{\theta} = arg \max_{\theta} \frac{1}{\sigma_{min}(\theta)} , \tag{27}$$

where $\sigma_{min}(\theta)$ is the shortest singular value of $D_i^{''}(\theta)$.

The output data of a DFT or bandpass filter is not necessarily an accurate narrowband signal. Moreover, the filtered signals may degrade DOA prediction performance. The TOPS approach may minimize these drawbacks by applying a particular signal subspace generated by the measured covariance matrix, rather than the steering array of the frequency range. This signifies that the approach used to select the range of frequencies from which the signal subspace is converted by Eq. (21) impacts the localization of wideband sources. On the other hand, the residual error of the subspaces results in certain unwanted rank reductions of the matrix $D_i^{''}(\theta)$. Consequently, TOPS suffers from a considerable limitation when it comes to generating certain spurious peaks in the spectrum simulated by Eq. (27).

4.6. S-TOPS Approach

To enhance DOA estimation performance, squared TOPS (S-TOPS) incorporates two strategies into the TOPS method. The first is to determine the frequency band from which the signal subspace will be employed. The other is a strategy to increase the sensitivity of reduction rank of the estimator $D_i^{''}(\theta)$ when θ is the desired DOA of the arriving broadband signals. The band of frequencies with the maximum SNR should operate as the reference frequency, which is considered to be the frequency range in which the signal subspace will be employed. S-TOPS employs the range of frequencies with the difference between the lowest signal eigen-value $\lambda_L(\omega_i)$ and the highest noise eigen-value $\lambda_(L+1)(\omega_i)$ is higher than in the reference frequency [22]. Then, Eq. (21) transforms the signal subspace of the reference range of frequencies into another range of frequency. Suppose that the range of frequencies ω_i is chosen, and the signal subspace $F_s(\omega_i)$ is converted into another frequency band ω_j. We generate the matrix $Q_i(\theta)$ for testing the squared orthogonality of projected subspaces using the converted signal subspace $U_{ij}^{'}(\theta)$ and the noise subspace $F_n(\omega_j)$, as follows:

$$Q_i(\theta) = \begin{bmatrix} U_{12}^{'H}F_n(\omega_2)F_n(\omega_2)^H U_{12}' \\ U_{13}^{'H}F_n(\omega_3)F_n(\omega_3)^H U_{13}' \\ \vdots \\ U_{1K}^{'H}F_n(\omega_K)F_n(\omega_K)^H U_{1K}' \end{bmatrix}^T . \tag{28}$$

Algorithm 6. S-TOPS algorithm.

1: Split the data into K blocks of the same size.
2: Calculate the DFT of the K blocks.
3: For $i = 1, 2, \ldots, K$ **do**
4: Select $x(\omega_i)$ at preselected ω_i.

5: Calculate the correlation matrix R_{xx} of every frequency ω_i.
6: End for
7: For $i = 1, 2, \ldots, K$ **do**
8: Calculate the signal subspace $F_s(\omega_1)$.
9: Compute the noise subspace $F_n(\omega_i)$ by EVD/SVD of the calculated correlation matrix R_{xx}.
10: Generate $D_i''(\theta)$ using Eqs. (25) and (26) for each hypothesized DOA θ.
11: Calculate the squared orthogonality of projected subspaces $Q_i(\theta)$ using Eq. (28) for each hypothesized DOA θ.
12: End for
13: Estimate the final DOA $\hat{\theta}$ by:

$$\hat{\theta} = arg \max_{\theta} \frac{1}{\sigma_{min}(\theta)}, \tag{29}$$

where $\sigma_{min}(\theta)$ is the shortest singular value of $Q_i(\theta)$.

When θ is the DOA of the arriving broadband signal, the row and column components of the matrix $Q_i(\theta)$ produced by the squared process should be close to zero. This demonstrates that the procedure enhances the sensitivity of estimating rank reduction of the orthogonality evaluation matrix. Hence, it improves the estimated resolution of S-TOPS. Nevertheless, the unwanted lobes in the spectra still exist.

5. Simulation Results

In this part, several simulations were run to evaluate the efficiency of these approaches. Matlab 2020a has been employed to demonstrate the performance of these approaches. The received data are split into $K = 256$ blocks, with the number of snapshots in each block equaling 100, using an ULA array of 10 sensors to show various scenarios. λ is the wavelength that refers to the center frequency ω_0. The signals share identical frequency bands. Table 1 shows the parameters used in the simulations.

Tab. 1. Simulation parameters.

Description	Symbols	Value
Antennas spacing	d	$\lambda/2$
Number of sources	L	3
Number of antennas	M	10
Smallest frequency	ω_S	2 MHz
Largest frequency	ω_L	4 MHz
Center frequency	ω_0	$(\omega_S + \omega_L)/2$
Nyquist sampling frequency	ω_{NS}	10 MHz

5.1. Spatial Spectrum

For each hypothesis, the spectra depict the results achieved with the use of the DOA estimation methods. The estimated

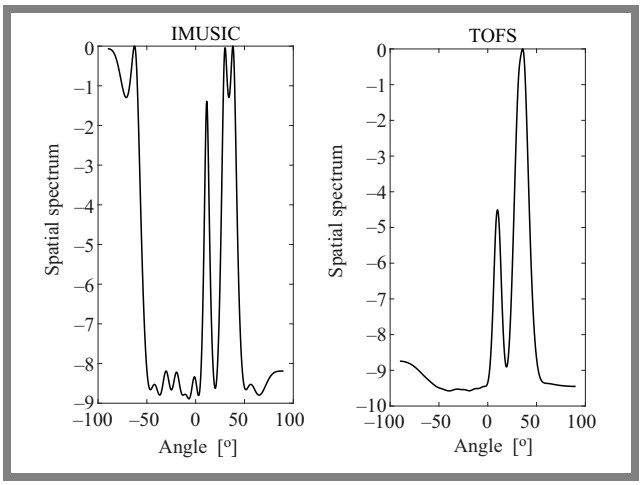

Fig. 2. Spatial spectra of the IMUSIC and TOFS algorithms at $M = 10$, $L = 3$ $(10°, 30°, 38°)$, and SNR $= 0$ dB.

DOAs are indicated by the peaks. For the simulation scenarios, Figs. 2, 3, and 4 depict the spatial spectra of all methods mentioned in this paper for a ten-sensor ULA. The spatial spectra are estimated at the angles of $\theta_1 = 10°$, $\theta_2 = 30°$, and $\theta_3 = 38°$ to illustrate the capabilities of each technique in a noisy environment with SNR = 0 dB. The sources are detected by all methods, which results in high peaks of real DOAs. TOFS, CSSM, and TCT eliminate all false peaks.
The spatial spectra indicate false lobes at erroneous angles that can be detected as DOAs using the TOPS and S-TOPS methods, as opposed to smaller peaks at true DOAs. The IMUSIC and TOFS techniques that can be used for reconstructing the arriving signals and TCT reach higher power values than the remaining approaches.

From Fig. 2, when SNR is 0 dB, it is clear that the TOFS algorithm is incapable of resolving the nearest sources (30°, 38°), while the IMUSIC method can detect the two closest sources. However, it suffers from side fluctuations at approx. $-60°$. Figure 3 indicates that all the estimation approaches have solved the true DOAs successfully, with some fake peaks generated between the calculated DOAs. Figure 4 illustrates the spectra of CSSM and TCT approaches, when SNR is 0 dB. TCT performs the best when SNR is low, without showing any false peaks, whereas CSSM cannot detect closely spaced signal sources (difference of 8°).

According to simulation results, TCT, TOPS, S-TOPS, and IMUSIC are capable of detecting two closely separated targets with a greater degree of precision in mid-to-high SNR conditions. TOPS and S-TOPS both help us improve average performance in the entire SNR range, with an advantage over other methods in low SNR, while S-TOPS shows small fake peaks compared with the TOPS algorithm.
In terms of simplicity, TOFS is similar to IMUSIC, however TOPS and S–TOPS still have significant computational costs due to the complicated calculations required. Note that CSSM and TCT methods require initial values.

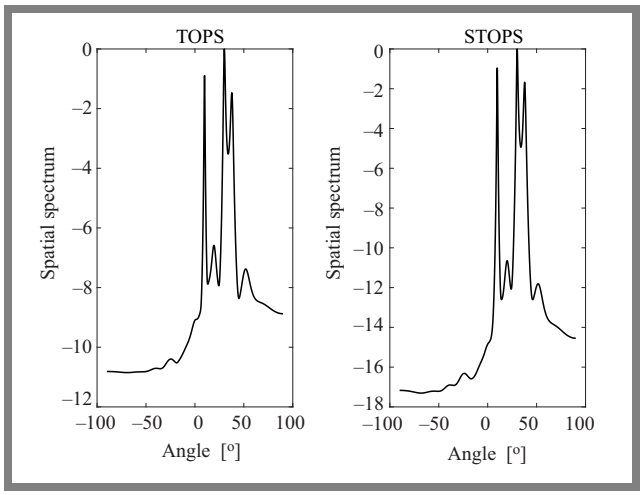

Fig. 3. Spatial spectra of the TOPS and S-TOPS algorithms at $M = 10$, $L = 3$ $(10°, 30°, 38°)$, and SNR $= 0$ dB.

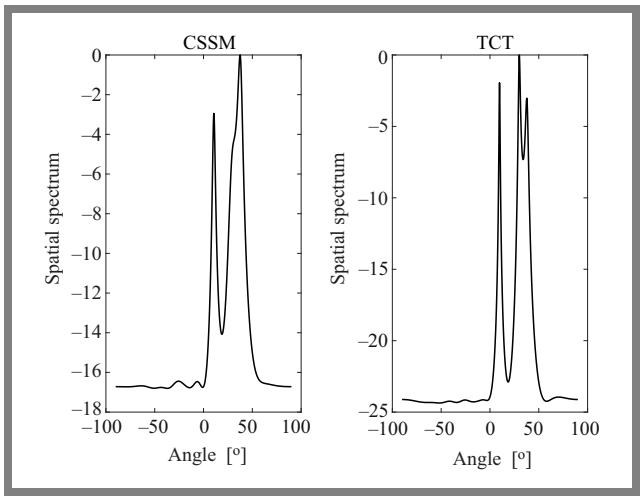

Fig. 4. Spatial spectra of the CSSM and TCT algorithms at $M = 10$, $L = 3$ $(10°, 30°, 38°)$, and SNR $= 0$ dB.

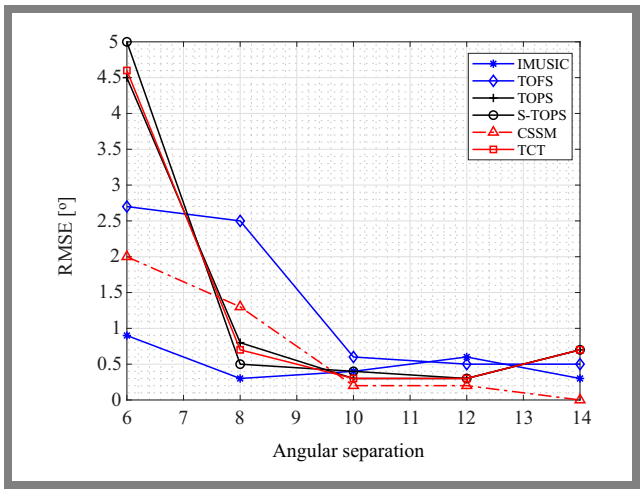

Fig. 5. RMSE against angular separation for SNR $= 0$ dB.

5.2. RMSE

For each simulation case, the root mean square error (RMSE) for the estimated DOAs of all sources is calculated as:

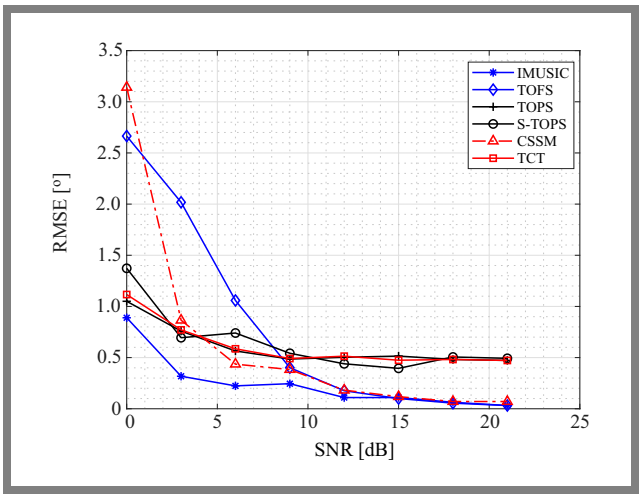

Fig. 6. RMSE versus SNR for the detected source $38°$.

$$\text{RMSE} = \sqrt{\frac{1}{PL}\sum_{l=1}^{L}\sum_{n=1}^{P}\left(\hat{\theta}_l(n) - \theta_l\right)^2}, \tag{30}$$

where θ_l is the l-th real DOA and $\hat{\theta}_l(n)$ is the l-th calculated DOA at every simulation trial, where the number of trials is $P = 10$. An average of the number of arriving signals is obtained in order to calculate the overall errors for all predicted DOAs.

Figure 5 shows RMSE plots for IMUSIC, TOFS, TOPS, S-TOPS, CSSM, and TCT algorithms for different angular separations, with a changing value of the signal source θ_3, with SNR being fixed – in this case at 0 dB – and the snapshot number equaling 100.

In Fig. 6, we examine the performance of IMUSIC, TOFS, TOPS, S-TOPS, CSSM, and TCT algorithms in terms of RMSE. Depicted in the Fig. 6 are the RMSE outcomes of the compared approaches versus SNR, where the average SNR ranges from 0 dB to 21 dB, and the snapshot number is 100. The associated DOA is $\theta = 38°$.

In terms of RMSE, TOPS and S-TOPS performed well across the entire range, while IMUSIC and TOFS performed similarly and outperformed the other algorithms in mid-to-high SNR ranges. IMUSIC achieves nearly the same performance as TOFS under good conditions ($SNR \geqslant 10$ dB). TOPS and S-TOPS provided average performance as the number of snapshots increased. With a high number of snapshots, IMUSIC and TOFS can effectively identify the right DOAs. As the angular separation varies, we consistently observe similar outcomes, with improved performance as the separation increases. Nevertheless, TOPS, S-TOPS, and TCT exhibit limitations when the angular separation between two signal sources is small.

6. Conclusion

This paper presents a detailed comparison of six high-resolution techniques used for calculating the DOA of wideband sources. For various SNR values, varied number of

snapshots and varied number of antennas, a comparison of six alternative methods for calculating DOA was provided. A ULA of ten antennas constitutes the receiver system. When the number of sources is known, computer simulations illustrate how well each algorithm performs. IMUSIC, TOPS, S-TOPS and TCT are capable of handling two closely spaced targets with a greater resolution in noisy environments (low SNR). With mid-to-high SNR values, TOFS, IMUSIC and CSSM perform best, whereas TOPS, S-TOPS and TCT show improved average performance in the entire SNR range. In the future, the authors will focus on deep/machine learning techniques to enhance the resolution of these approaches.

References

[1] S. Ebihara, Y. Kimura, T. Shimomura, R. Uchimura, and H. Choshi, "Coaxial-fed circular dipole array antenna with ferrite loading for thin directional borehole radar sonde", *IEEE Transactions on Geoscience and Remote Sensing*, vol. 53, no. 4, pp. 1842–1854, 2015 (https://doi.org/10.1109/TGRS.2014.2349921).

[2] U. Nielsen and J. Dall, "Direction-of-arrival estimation for radar ice sounding surface clutter suppression", *IEEE Transactions on Geoscience and Remote Sensing*, vol. 53, no. 9, pp. 5170–5179, 2015 (https://doi.org/10.1109/TGRS.2015.2418221).

[3] R. Takahashi, T. Inaba, and T. Takahashi, "Digital Monopulse Beamforming for Achieving the CRLB for Angle Accuracy", *IEEE Transactions on Aerospace and Electronic Systems*, vol. 54, no. 1, pp. 315–323, 2018 (https://doi.org/10.1109/TAES.2017.2756519),

[4] B. Cantrell, J. Rao, G. Tavik, and V. Krichevsky, "Wideband array antenna concept", in *IEEE International Radar Conference*, Arlington, USA, pp. 680–684, 2005 (https://doi.org/10.1109/MAES.2006.1581120).

[5] Z.M. Liu, Z.T. Huang, and Y.Y. Zhou, "Direction-of-Arrival Estimation of Wideband Signals via Covariance Matrix Sparse Representation", *IEEE Transactions on Signal Processing*, vol. 59, no. 9, pp. 4256–4270, 2011 (https://doi.org/10.1109/TSP.2011.2159214).

[6] A. Toktas and A. Akdagli, "Compact multiple-input multiple-output antenna with low correlation for ultra-wideband applications", *IET Microwaves, Antennas and Propagation*, vol. 9, no. 8, pp. 822–829, 2015 (https://doi.org/10.1049/iet-map.2014.0086).

[7] M. Frikel, S. Safi, and Y. Khmou, "Focusing Operators and Tracking Moving Wideband Sources", *Journal of Telecommunications and Information Technology*, no. 4, pp. 53–59, 2016 (https://www.itl.waw.pl/czasopisma/JTIT/2016/4/53.pdf).

[8] I. Atanasov, A. Nikolov, and E. Pencheva, "An approach to transform Internet of Things data into knowledge", *International Journal of Embedded Systems*, vol. 9, no. 5, pp. 401–412, 2017 (https://doi.org/10.1504/IJES.2017.086722).

[9] P. Thanapal and M.A.S. Durai, "A framework for computational offloading to extend the energy of mobile devices in mobile cloud computing", *International Journal of Embedded Systems*, vol. 9, no. 5, pp. 444–455, 2017 (https://doi.org/10.1504/IJES.2017.086725).

[10] S. Narendrakumar *et al.*, "Token security for Internet of Things", *International Journal of Embedded Systems*, vol. 10, no. 4, pp. 334–343, 2018 (https://doi.org/10.1504/IJES.2018.093689).

[11] H. Ougraz, S. Safi, and M. Frikel, "Analysis of Several Algorithms for DOA Estimation in Two Different Communication Models by a Comparative Study", *Lecture Notes in Business Information Processing*, vol. 449, pp. 219–230, 2022 (https://doi.org/10.1007/978-3-031-06458-6_18).

[12] J. Zhang, J. Dai, and Z. Ye, "An extended TOPS algorithm based on incoherent signal subspace method", *Signal Processing*, vol. 90, no. 12, pp. 3317–3324, 2010 (https://doi.org/10.1016/j.sigpro.2010.05.031).

[13] H. Hayashi and T. Ohtsuki, "DOA estimation for wideband signals based on weighted squared TOPS", *EURASIP Journal on Wireless Communications and Networking*, no. 1, pp. 1–12, 2016 (https://doi.org/10.1186/s13638-016-0743-9).

[14] H. Hung and M. Kaveh, "Focussing matrices for coherent signal subspace processing", *IEEE Transactions on Acoustics, Speech, and Signal Processing*, vol. 36, no. 8, pp. 1272–1281, 1998 (https://doi.org/10.1109/29.1655).

[15] Z. Ahmad, Y. Song, and Q. Du, "Wideband DOA estimation based on incoherent signal subspace method", *COMPEL International Journal for Computation and Mathematics in Electrical and Electronic Engineering*, vol. 37, no. 8, pp. 1271–1289, 2018 (https://doi.org/10.1108/COMPEL-10-2017-0443).

[16] H. Wang and M. Kaveh, "Coherent signal-subspace processing for the detection and estimation of angles of arrival of multiple wideband sources", *IEEE Transactions on Acoustics, Speech, and Signal Processing*, vol. 33, no. 4, pp. 823–831, 1985 (https://doi.org/10.1109/TASSP.1985.1164667).

[17] K.S. Huang, Y.Y. Zhou, and G.Z. Zhang, "A fast DOA estimating method of wideband signals based on Krylov subspace", *Journal of Astronautics*, vol. 26, no. 4, pp. 461–465, 2005.

[18] M. Wax, T.J. Shan, and T. Kailath, "Spatio-temporal spectral analysis by eigenstructure methods", *IEEE Transactions on Acoustics, Speech, and Signal Processing*, vol. 32, no. 4, pp. 817–827, 1984 (https://doi.org/10.1109/TASSP.1984.1164400).

[19] R. Schmidt, "Multiple emitter location and signal parameter estimation", *IEEE Transactions on Antennas Propagation*, vol. 34, no. 3, pp. 276–280, 1986 (https://doi.org/10.1109/TAP.1986.1143830).

[20] H. Yu, J. Liu, Z. Huang, Y. Zhou, and X. Xu, "TOFS: A new method for wideband DOA estimation", in *2007 International Conference on Wireless Communications, Networking and Mobile Computing*, vol. 28, Shanghai, China, pp. 598–601, 2007 (https://doi.org/10.1109/WICOM.2007.155).

[21] Y.S. Yoon, L.M. Kaplan, and J.H. McClellan, "TOPS: new DOA estimator for wideband signals", *IEEE Transactions on Signal Processing*, vol. 54, no. 6, pp. 1977–1989, 2006 (https://doi.org/10.1109/TSP.2006.872581).

[22] K. Okane and T. Ohtsuki, "Resolution Improvement of Wideband Direction-Of-Arrival Estimation Squared-TOPS", in *2010 IEEE International Conference on Communications*, Cape Town, South Africa, pp. 1–5, 2010 (https://doi.org/10.1109/ICC.2010.5502480).

[23] M.A. Doron and A.J. Weiss, "On focusing matrices for wide-band array processing", *IEEE Transactions on Signal Processing*, vol. 40, no. 6, pp. 1295–1302, 1992 (https://doi.org/10.1109/78.139236).

[24] F. Sellone, "Robust auto-focusing wideband DOA estimation", *Signal Processing*, vol. 86, no. 1, pp. 17–37, 2006 (https://doi.org/10.1016/j.sigpro.2005.04.009).

[25] D.N. Swingler and J. Krolik, "Source location bias in the coherently focused high-resolution broadband beamformer", *IEEE Transactions on Acoustics, Speech, and Signal Processing*, vol. 37, no. 1, pp. 143–145, 1989 (https://doi.org/10.1109/29.17516).

[26] P.J. Chung, J.F. Bohme, C.F. Mecklenbrauker, and A.O. Hero, "Detection of the number of signals using the Benjamini-Hochberg procedure", *IEEE Transactions on Signal Processing*, vol. 55, no. 6, pp. 2497–2508, 2007 (https://doi.org/10.1109/TSP.2007.893749).

[27] H. Wang and M. Kaveh, "Coherent signal-subspace processing for the detection and estimation of angles of arrival of multiple wideband sources", *IEEE Transactions on Acoustics, Speech, and Signal Processing*, vol. 33, no. 4, pp. 823–831, 1985 (https://doi.org/10.1109/TASSP.1985.1164667).

[28] S. Valaee and P. Kabal, "Wideband array processing using a two-sided correlation transformation", *IEEE Transactions on Signal processing*, vol. 43, no. 1, pp. 160–172, 1995 (https://doi.org/10.1109/78.365295).

[29] Y. Zeng and G. Lu, "Efficient wideband signals direction of arrival estimation method with unknown number of signals", *International Journal of Distributed Sensor Networks*, vol. 12, no. 11, 2016 (https://doi.org/10.1177/1550147716676557).

[30] A. Asadzadeh, S.M. Alavi, M. Karimi, and H. Amiri, "Coherent wide-band signals DOA estimation by the new CTOPS algorithm", *Multidimensional Systems and Signal Processing*, vol. 31, pp. 1075–1089, 2020 (https://doi.org/10.1007/s11045-020-00699-z).

Hassan Ougraz, M.Sc.
Department of Mathematics and Computer Sciences, LIMATI Laboratory
https://orcid.org/0000-0002-0450-4893
E-mail: hassan.ougraz.24@gmail.com
University of Sultan Moulay Slimane Beni Mellal, Morocco
https://www.usms.ac.ma

Said Safi, Ph.D., Professor
Department of Mathematics and Computer Sciences
https://orcid.org/0000-0003-3390-9037
University of Sultan Moulay Slimane Beni Mellal, Morocco
https://www.usms.ac.ma

Ahmed Boumezzough, Ph.D., Professor
Applied Physics and New Technologies Team
E-mail: ahmed.boumezzough@gmail.com
University of Sultan Moulay Slimane Beni Mellal, Morocco
https://www.usms.ac.ma

Miloud Frikel, Ph.D., Professor
Department of Physics
https://orcid.org/0000-0003-2178-1814
National Graduate School of Engineering and Research Center Caen, France
https://www.ensicaen.fr